IEEE Photonics Journal
An IEEE Photonics Society Publication

Open Access

Injection-Locked Millimeter Wave Frequency Divider Utilizing Optoelectronic Oscillator Based Optical Frequency Comb

Volume 11, Number 3, June 2019

Yongchi Xu
Huanfa Peng
Rui Guo
Huayang Du
Qing Yin
Guoqing Hu
Jin He
Zhangyuan Chen

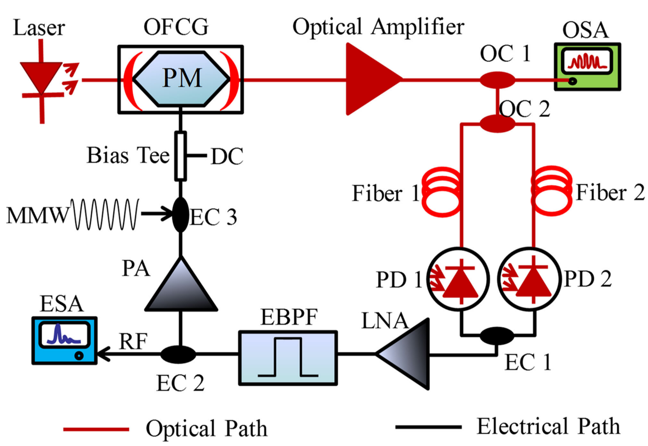

DOI: 10.1109/JPHOT.2019.2916919

Injection-Locked Millimeter Wave Frequency Divider Utilizing Optoelectronic Oscillator Based Optical Frequency Comb

Yongchi Xu,[1] Huanfa Peng,[1] Rui Guo,[1] Huayang Du,[1] Qing Yin,[1] Guoqing Hu,[2] Jin He,[2] and Zhangyuan Chen[1,2]

[1]State Key Laboratory of Advanced Optical Communication Systems and Networks, Department of Electronics, Peking University, Beijing 100871, China
[2]Peking University Shenzhen Institution, Shenzhen 518055, China

DOI:10.1109/JPHOT.2019.2916919

Manuscript received April 24, 2019; accepted May 11, 2019. Date of publication May 14, 2019; date of current version June 3, 2019. This work was supported in part by the National Natural Science Foundation of China under Grants 61690194, 61805003, and 61505002; in part by the China Postdoctoral Science Foundation under Grant 2018M630035; and in part by the Fundamental Research Project of Shenzhen Science and Technology Fund under Grants JCYJ20170307172513653, JCYJ20170412153812353, JCYJ20170307164201104, JCYJ20170817113758285, and JCYJ20170817112527562. Corresponding author: Zhangyuan Chen (e-mail: chenzhy@pku.edu.cn).

Abstract: We propose and experimentally demonstrate a photonic millimeter-wave frequency divider based on a super-harmonic injection-locked optoelectronic oscillator (OEO) and an optical frequency comb. The optical frequency comb generator is incorporated into an OEO loop to create broadband comb lines with low noise. By injecting a millimeter-wave with frequency around *N* times of the fundamental oscillating frequency f_0 of the OEO, the injection signal can be down-converted to an intermediate frequency (IF) signal close to the oscillating frequency of the OEO. The free running OEO is synchronized with the IF signal via an injection locking mechanism. Consequently, it forms an injection-locked frequency divider as the frequency ratio between the injection signal and OEO's output signal is precisely equal to *N*. We carry out an experiment to divide the 45 GHz signal into 7.5 GHz and the experimental results agree well with the theoretical analysis. By changing the frequency of the injection signal, division ratio from 2 to 5 is also demonstrated on one setup. Due to the broadband spectra of the optical comb and low phase noise characteristics of the OEO, it is potential to realize very large division ratio and low phase noise for multiple input frequencies mf_0.

Index Terms: Optoelectronic oscillator, injection-locked frequency divider, optical frequency comb.

1. Introduction

As an integral part of the phase-locked loop (PLL), the frequency divider is one of the key components in millimeter-wave applications, such as radar, communication and metrology [1]–[3]. One divider or multi-stage divider is used in a PLL to frequency down-convert the free running multi-GHz waveforms, so as to stabilize them with a fixed, ultra-stable and low-frequency reference [2]. There are two types of frequency divider, namely the digital divider and analog divider. The

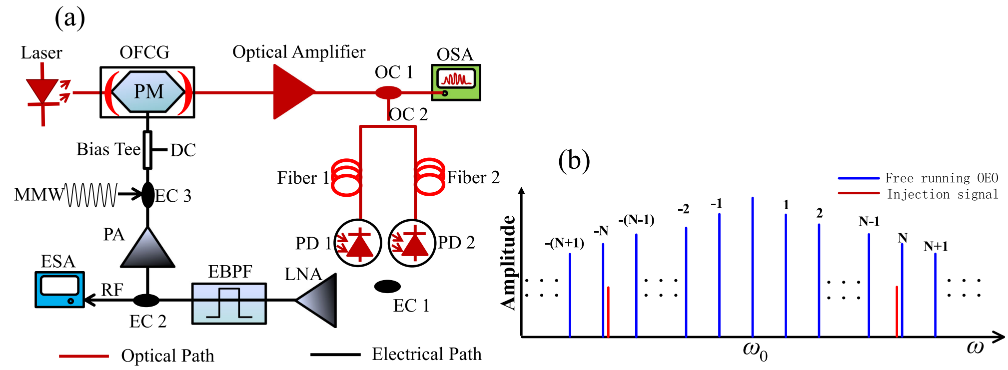

Fig. 1. (a) The schematic diagram of the proposed frequency divider. (b) The optical spectra of the free running OEO and that of the injection signal; OFCG: optical frequency comb generator; PM: phase modulator; OC: optical coupler; PD: photodiodes; EC: electrical coupler; EBPF: electrical bandpass filter; LNA: low noise amplifier; PA: power amplifier; MMW: millimeter-wave; DC: direct current; OSA: optical spectrum analyzer; ESA: electrical spectra analyzer.

working bandwidth of the digital frequency divider is limited to several GHz while that of the analog frequency divider can be up to tens of GHz [2], [4], [5]. Besides, analog dividers have lower phase noise [4]. As a result, analog dividers are widely used as the prescaler in millimeter-wave PLLs. However, it is challenging to get a large division ratio for high frequency application. Several schemes of injection-locked frequency dividers have been proposed for large division ratios [6]–[8].

Recently, photonic-assisted approaches are proposed to realize optical frequency division [9]–[11] and microwave frequency division [12]–[15]. Among them, the OEOs were used to achieve microwave frequency division [13]–[15], which have the potential to obtain the large frequency division ratio and low phase noise, simultaneously. In [13], a 20 GHz frequency divider with a division factor of 2 was reported based on a super-harmonic injection locked OEO. In [14], a 24 GHz frequency divider with variable division ratio was demonstrated. In [15], a wideband microwave frequency divider based on an OEO was demonstrated. By using carrier-suppressed optical double sideband (CS-ODSB) modulation, a frequency division ratio of 2 was realized. However, it is hard to achieve a large division ratio by these methods.

In this paper, we demonstrate a millimeter-wave frequency divider with large division ratio via a super-harmonic injection-locked OEO and an optical frequency comb generator (OFCG). In order to divide the millimeter-wave signal into a signal with lower frequency, we inject it into a free-running OEO. The frequency of the injected millimeter-wave is close to integer-N times of the OEO's oscillating frequency. We put an OFCG in the OEO loop, so that the optical spectrum is wide enough to cover the *Nth* modulation sideband of the OEO. In this case, after injecting the millimeter-wave signal into the OEO, the OEO's oscillating frequency can be synchronized with the millimeter-wave signal when the OEO is injection-locked. The injection-locked OEO forms a frequency divider. Experimentally, we divide 5 input frequencies, from 15 GHz to 45 GHz, into a 7.5 GHz signal on one single-stage setup, corresponding to division ratios of 2 to 6. We also investigate the noise characteristics of this super-harmonic injection locked OEO. The measured results agree well with our theoretical predictions. Compared with the previous reported OEO based injection-locked frequency dividers, due to the broadband optical spectra, this photonic frequency divider has great potential to obtain an ultra-large division ratio. Besides, with the progress of the integrated broadband electro-optic frequency comb [16] and OEO [17], our scheme can be realized on a chip-scale platform in the near future. By using integration techniques, the power consumption of the proposed frequency divider can be reduced.

2. Operation Principle

Fig. 1(a) shows the schematic diagram of our proposed millimeter-wave frequency divider. We apply the injection-locked mechanism [18]–[20] to synchronize the OEO and the millimeter-wave signal. As shown in Fig. 1(a), we inject the input signal into a dual-loop OEO [21], [22]. The frequency of the injection signal is around N times of the oscillating frequency of the OEO. An optical frequency comb generator is placed in the OEO as a modulator. When the frequency of the OEO is integer-multiples of the free-spectral-range (FSR) of the OFCG [21], it generates multiple optical comb lines, as shown by the blue lines in Fig. 1(b). Meanwhile, the injection signal can also create modulation sidebands through the OFCG, as shown by the red lines in Fig. 1(b). After photo-detection, a beat-note between the modulation sidebands of injection signal and the $(N \pm 1)$th sidebands of the free-running OEO can be generated. The frequency of the beat-note is close to that of the OEO. If it locates at the locking range, the OEO locks onto the injection millimeter-wave signal. After injection-locked, the frequency of the OEO is $1/N$ of the frequency of the injection millimeter-wave signal. It forms a divide-by-N frequency divider.

In order to investigate the locking range and phase noise performance of this frequency divider, theoretical analysis is given in the following part.

By assuming the detuning frequency between the seed laser and the cavity resonance is 0, and the single-pass power transmission efficiency is 100%, the output electrical field of the OFCG can be expressed as [23]

$$E_{OUT} \approx \frac{1-R}{1-R\exp\left[-i\beta_1 \sin\left(\omega_{OEO}t\right)\right]\cdot\exp\left[-i\beta_2\sin\left(\omega_{INJ}t\right)\right]}E_0, \tag{1}$$

where R is the power reflection coefficient of the F-P facet coating in the OFCG, β_1 and β_2 are the modulation index of the OFCG driven by the OEO and the injection signal, E_0 is the electrical field of the seed laser, ω_{OEO} and ω_{INJ} are the angular frequency of the free-running OEO and the injection signal. We have the condition of $\omega_{INJ} \approx N\omega_{OEO}$.

The optical intensity of the output of OFCG is

$$P_{OUT} = E_{OUT}\cdot E^*_{OUT}. \tag{2}$$

By substituting Eq. (1) into Eq. (2), the optical intensity can be derived and be expanded by Taylor series as

$$P_{OUT} \approx \frac{(1-R)^2\cdot P_0}{2}\cdot\left(1+R\cos\gamma+R^2\cos^2\gamma+R^3\cos^3\gamma\cdots\right), \tag{3}$$

where P_0 is the optical power injecting to the OFCG. The parameter of γ is defined as $\gamma = \beta_1\sin\left(\omega_{OEO}t\right)+\beta_2\sin\left(\omega_{INJ}t\right)$. The term of $\cos\gamma$ in Eq. (3) includes the intermodulation components between the OEO and the injection signal. It can be derived as

$$\begin{aligned} U(t) = {} & 4\sum_{m=1}^{\infty}\sum_{n=1}^{\infty}J_{2m}(\beta_1)J_{2n}(\beta_2)\cos\left[2m\cdot\omega_{OEO}t\right]\cos\left[2n\cdot\omega_{INJ}t\right] \\ & -4\sum_{m=1}^{\infty}\sum_{n=1}^{\infty}J_{2m-1}(\beta_1)J_{2n-1}(\beta_2)\sin\left[(2m-1)\cdot\omega_{OEO}t\right]\sin\left[(2n-1)\cdot\omega_{INJ}t\right], \end{aligned} \tag{4}$$

where J_n is the n-th Bessel function of the first kind. The free-running OEO can be injection-locked by the intermodulation components with the frequency close to the OEO. Here, we derive it as

$$u(t) = 2J_1(\beta_2)\cdot J_{N-1}(\beta_1)\cdot\cos\left\{\left[\omega_{INJ}-(N-1)\omega_{OEO}\right]t\right\}, \tag{5}$$

Note that due to the power of the $(N+1)$th sidebands are lower than that of the $(N-1)$th sidebands, we neglect the intermodulation component between the $(N+1)$ order harmonics of the OEO and the fundamental frequency of the injection signal. Consequently, the photocurrent of the intermodulation component in Eq. (5) can be expressed as

$$I_{ph} \approx \eta\cdot\frac{(1-R)^2\cdot P_0}{2}\cdot R\cdot 2J_1(\beta_2)\cdot J_{N-1}(\beta_1)\cdot\cos\left\{\left[\omega_{INJ}-(N-1)\omega_{OEO}\right]t\right\}, \tag{6}$$

where η is the responsibility of the PD. The intermodulation component in Eq. (6) can be regarded as an IF down-converted from the millimeter-wave signal. According to the Paciorek's equation [24], the locking range of the free-running OEO can be described as

$$\Delta\omega_{lock} = (\omega_{OEO}/2Q) \cdot (\varepsilon/\sqrt{1-\varepsilon^2}), \tag{7}$$

where $\varepsilon = \sqrt{P_{INJ}/P_{OEO}}$. P_{INJ} is the power of the IF signal down-converted from the injection signal, which can be calculated by $P_{INJ} = I_{ph}^2 \cdot Z$. Z is the impedance of the photodiode, P_{OEO} is the power of the free-running OEO at the output of PD, Q is the quality factor of the OEO. If the frequency of the intermodulation component is within the locking range, then the OEO can be synchronized with the injection signal. So that the angular frequency of the OEO and the injection signal satisfies the following condition

$$\omega_{INJ} - (N-1)\omega_{OEO} = \omega_{OEO}. \tag{8}$$

The Eq. (8) can be simplified as

$$\omega_{OEO} = \frac{1}{N}\omega_{INJ}. \tag{9}$$

According to Eq. (9), we can conclude that the injection-locked OEO forms a divide-by-N frequency divider. Furthermore, the phase noise performance of this frequency divider can be evaluated by [25]

$$\mathcal{L}_{ILO}(f) = \frac{(1/N)^2 \cdot K_{ILO}^2}{(2\pi f)^2 + K_{ILO}^2} \cdot \mathcal{L}_{INJ}(f) + \frac{(2\pi f)^2}{(2\pi f)^2 + K_{ILO}^2} \cdot \mathcal{L}_{OEO}(f), \tag{10}$$

where f is the Fourier frequency offset, and the K_{ILO} is defined as

$$K_{ILO} = \frac{\varepsilon^2 + \varepsilon\cos(\varphi)}{(1+\varepsilon \cdot \cos(\varphi))^2}\frac{\omega_{OEO}}{2Q}, \tag{11}$$

where φ is the fixed phase difference between the IF and the injection-locked OEO, which is defined as $\varphi = \arcsin(\Delta\omega_0/\Delta\omega_{lock})$ [18]. $\Delta\omega_0$ is the angular frequency difference between the free-running OEO and the IF before injection-locked. From Eq. (10), we can infer that at the offset within the locking bandwidth, the phase noise can decrease by $20\log_{10}(N)$ dB. It leads to the long-term stability of the frequency-divided output signal dominated by the frequency stability of the injection signal. While out of the locking bandwidth, the phase noise of the divider output is mainly determined by the OEO.

3. Experimental Details and Results

We carry out an experiment based on the setup showing in Fig. 1(a). The center wavelength of the seed laser is 1550 nm. The FSR of the optical frequency comb generator is 2.5 GHz. The coupling ratio of optical couplers 1 and 2 are 10:90 and 50:50. The lengths of the two fibers are 2 m and 100 m. The bandwidth of the photodiode in use is 10 GHz. The center frequency of the electrical band-pass filter is 7.5 GHz. The coupling ratio of electrical couplers 1, 2, and 3 are 50:50, 10:90, and 50:50. The injection millimeter-wave signal is generated by a commercial frequency synthesizer. The power of the injection signal is about 4 dBm.

An optical comb with triangular-profile spectra is obtained, as shown in Fig. 2. The repetition rate is 7.5 GHz. After injecting a 45-GHz signal, the amplitudes of the 6th sidebands are higher than that of the free running OEO, like the red curve in Fig. 2. The output of the frequency divider is monitored by an electrical spectrum analyzer at one output port of the EC 2. Fig. 3(a) shows 5 input injection signals with frequencies from 15 GHz to 45 GHz, and the output 7.5 GHz signal, corresponding to division ratio of 2 to 6. It is potential to realize higher operation frequency when a larger modulation bandwidth of OFCG is used.

Locking range is one of the key parameters of the injection-locked frequency divider. To verify the locking range of our photonic frequency divider, we slightly tune the frequency of the injection signal, meanwhile, keeping the locking state. Fig. 3(b) presents the maximum tuning range of the injection-locked OEO. Correspondingly, the locking range is 20 kHz. In fact, this result is in agreement with

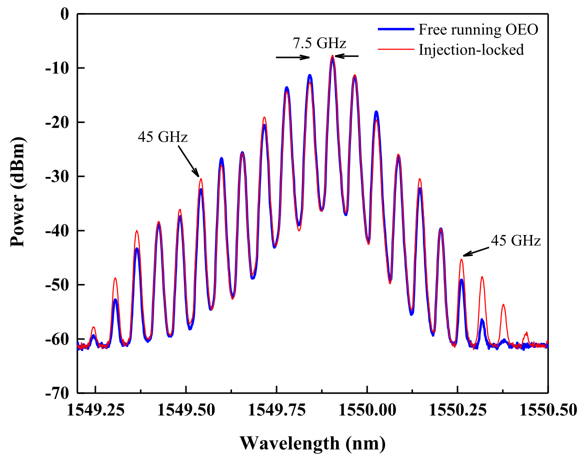

Fig. 2. The measured optical spectrum of the free running OEO and that of injection locked by 45 GHz signal.

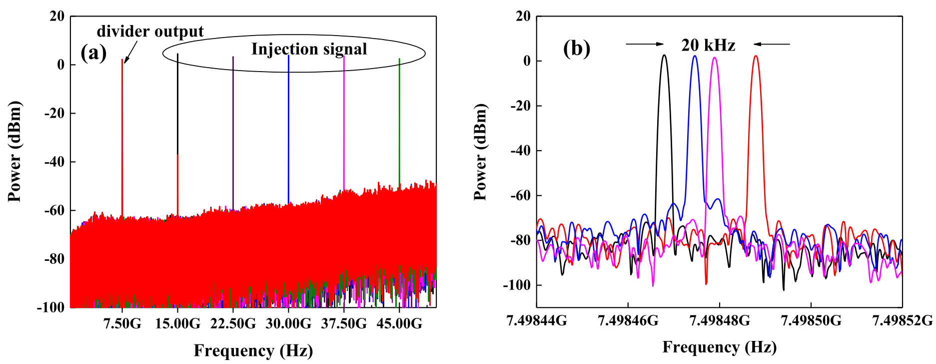

Fig. 3. Measured electrical spectra of (a) the divider output by injection signals with the frequency of 2–6 times of the 7.5 GHz-OEO. (b) The lock range of the 45 GHz-frequency divider with a division ratio of 6.

the theoretical estimation. According to Eq. (7) and experiment conditions, $\varepsilon = \sqrt{P_{INJ}/P_{OEO}} \approx 0.03$, $Q \approx 2.3 \times 10^4$, in our system, the estimated locking range is around 25 kHz. Within the locking range, the operation frequency of this photonic microwave frequency divider can be continuously tuned. We can further enlarge the locking range by decreasing the Q value of OEO or by increasing the injection ratio.

To confirm the injection-locked state, we measured the transient response of this frequency divider. Fig. 4(a) and (b) show the evolution of the frequency and phase of the OEO during the injection locking process. The measurement time is 20 ms. Due to the long-term stability of the injection signal is better than that of the free-running OEO, the frequency fluctuation of the OEO decreases after injection-locked, as shown in Fig. 4(a). The locking-time is about 200 us. Besides, the phase experiences an abrupt change during the locking process, as shown in Fig. 4(b).

We also measure the single-sideband phase noise of the 45 GHz injection signal, the free-running OEO, and the injection-locked OEO, as illustrated in Fig. 5. To investigate the phase noise performance of our proposed frequency divider, we use Eq. (10) to calculate the phase noise of the injection-locked OEO, as shown by the green curve. In this calculation, we substitute the experimental phase noise results of the injection millimeter-wave signal and OEO into Eq. (10). The frequency division ratio is set to 6. The locking bandwidth is 20 kHz, which is estimated by Eq. (11). Within the locking bandwidth, the phase noise is about 15 dB lower than that of the injection

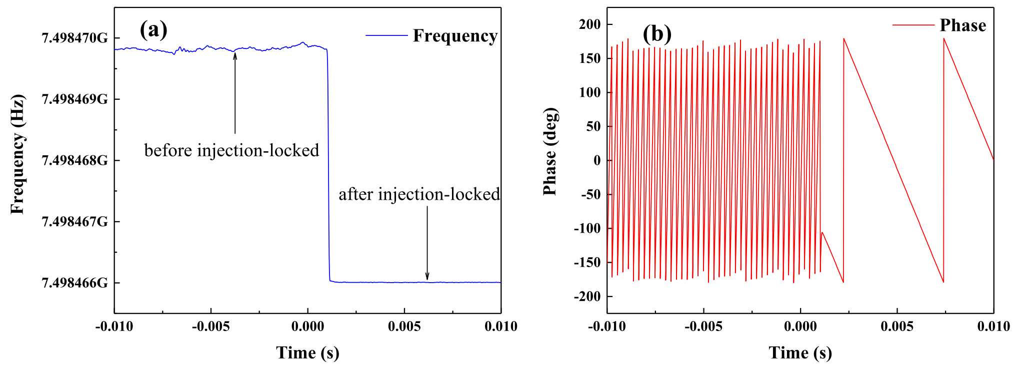

Fig. 4. The transient response of the injection-locked frequency divider. (a) The frequency, and (b) the phase change before and after injection.

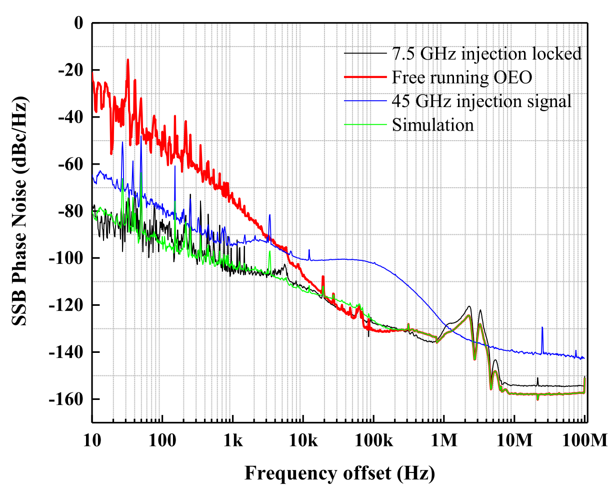

Fig. 5. The SSB phase noise comparison between the free-running OEO, the injection signal, the super-harmonic injection-locked OEO and the simulation result.

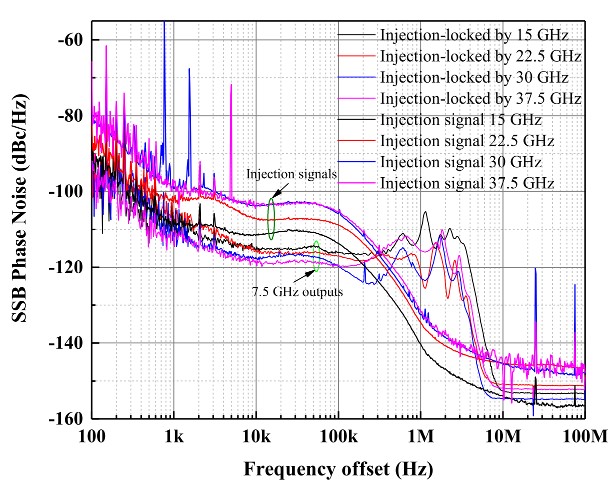

Fig. 6. The SSB phase noise of the 7.5 GHz output of the injection-locked OEOs for different injection signals from 15 to 37.5 GHz.

signal. This result agrees well with the theoretical calculation (20log10(6) = 15.6 dB). While beyond the locking bandwidth, the phase noise of the divider output is mainly determined by the OEO. The spurs around the offsets of 2 MHz and 4 MHz are induced by the side-modes of the OEO. Due to the low noise characteristic of the OEO, beyond the locking bandwidth, the proposed frequency divider can have lower phase noise than that of those conventional frequency dividers.

To investigate the phase noise of the output of the frequency divider with different injection signals, we also measure the SSB phase noise of different injection-locked OEOs (Indicated as the green circle) and the injection signals (Indicated as the olive circle), as shown in Fig. 6. The frequency of the injection signals is from 15 to 37.5 GHz with a step of 7.5 GHz. For each injection signal, the corresponding injection-locked OEO output suffers a phase noise decrease given by $20\log_{10}(N)$ at the frequency offset below 100 kHz. This trend is in agreement with the phase noise model in Eq. (10).

4. Conclusion

In summary, we have demonstrated a novel millimeter-wave frequency divider to overcome the division ratio limitation via a photonic approach. We use an injection-locked OEO to synchronize the millimeter-wave and the optical comb. The repetition rate of the optical comb is a fractional of the frequency of the millimeter-wave. Due to the broadband optical spectra of the optical comb, an ultra- large division ratio can be achieved. The phase noise decreasing in the locking range satisfies the relationship $20\log_{10}(N)$ between the injection signal and the output signal. Out of the locking range, the phase noise performance benefits from the OEO's low phase noise. Additionally, the frequency divider can divide multiple input frequencies ($N f_0$) into the fundamental oscillating frequency (f_0) of the OEO by one single-stage setup. In the future, a variable division ratio can be realized by a tunable OEO [26].

Acknowledgment

The authors would like to thank X. Xie for useful comments on this manuscript.

References

[1] M. Tiebout, "A CMOS direct injection-locked oscillator topology as high-frequency low-power frequency divider," *IEEE J. Solid-State Circuits*, vol. 39, no. 7, pp. 1170–1174, Jul. 2004.

[2] K. Yamamoto and M. Fujishima, "70 GHz CMOS harmonic injection-locked divider," in *Proc. Int. Conf. IEEE Solid State Circuits*, San Francisco, CA, USA, 2006, pp. 2472–2481.

[3] H. R. Rategh, H. Samavati, and T. H. Lee, "A CMOS frequency synthesizer with an injection-locked frequency divider for a 5-GHz wireless LAN receiver," *IEEE J. Solid-State Circuits*, vol. 35, no. 5, pp. 780–787, May 2000.

[4] E. Rubiola, M. Olivier, and J. Groslambert, "Phase noise in the regenerative frequency dividers," *IEEE Trans. Instrum. Meas.*, vol. 41, no. 3, pp. 353–360, Jun. 1992.

[5] H. C. Luong and J. Yin, *Transformer-Based Design Techniques for Oscillators and Frequency Dividers*. Berlin, Germany: Springer, 2015.

[6] S. Lee *et al.*, "A 37-GHz-input divide-by-36 injection-locked frequency divider with 1.6-GHz lock range," in *Proc. Asian Conf. IEEE Solid-State Circuits*, Tainan, Taiwan, 2018, pp. 219–222.

[7] P. Mayr, C. Weyers, and U. Langmann, "A 90 GHz 65 nm CMOS injection-locked frequency divider," in *Proc. Int. Conf. IEEE Solid-State Circuits*, San Francisco, CA, USA, 2007, pp. 198–596.

[8] S. Li, H. Yeh, and H. Chang, "A V-band 90-nm CMOS divide-by-10 injection-locked frequency divider using current-reused topology," *IEEE Microw. Wireless Compon. Lett.*, vol. 28, no. 1, pp. 76–78, Jan. 2018.

[9] T. M. Fortier *et al.*, "Generation of ultrastable microwaves via optical frequency division," *Nature Photon.*, vol. 5, no. 7, pp. 425–429, Jun. 2011.

[10] J. Li, X. Yi, H. Lee, S. A. Diddams, and K. J. Vahala, "Electro-optical frequency division and stable microwave synthesis," *Science*, vol. 345, no. 6194, pp. 309–313, Jul. 2014.

[11] X. Xie *et al.*, "Photonic microwave signals with zeptosecond-level absolute timing noise," *Nature Photon.*, vol. 11, no. 1, pp. 44–47, Jan. 2017.

[12] S.-C. Chan and J.-M. Liu, "Microwave frequency division and multiplication using an optically injected semiconductor laser," *IEEE J. Quantum Electron.*, vol. 41, no. 9, pp. 1142–1147, Sep. 2005.

[13] H. Peng *et al.*, "Low phase noise 20 GHz microwave frequency divider based on a super-harmonic injection locked optoelectronic oscillator," in *Proc. Int. Symp. IEEE Freq. Control*, Olympic Valley, CA, USA, 2018, pp. 1–3.

[14] H. Peng *et al.*, "Microwave frequency divider with variable dividing ratio based on a tunable optoelectronic oscillator," in *Proc. SPIE 10th Int. Conf. Inf. Opt. Photon.*, Beijing, China, 2018, pp. 1–5.
[15] S. Liu *et al.*, "Wideband microwave frequency division based on an optoelectronic oscillator," *IEEE Photon. Technol. Lett.*, vol. 31, no. 5, pp. 389–392, Mar. 2019.
[16] M. Zhang *et al.*, "Broadband electro-optic frequency comb generation in a lithium niobate microring resonator," *Nature*, vol. 568, pp. 373–377, Mar. 2019.
[17] M. Merklein *et al.*, "Widely tunable, low phase noise microwave source based on a photonic chip," *Opt. Lett.*, vol. 41, no. 20, pp. 4633–4636, Oct. 2016.
[18] R. Adler, "A study of locking phenomena in oscillators," *Proc. IRE*, vol. 34, no. 6, pp. 351–357, Jun. 1946.
[19] H. R. Rategh and T. H. Lee, "Superharmonic injection-locked frequency dividers," *IEEE J. Solid-State Circuits*, vol. 34, no. 6, pp. 813–821, Jun. 1999.
[20] B. Razavi, "A study of injection locking and pulling in oscillators," *IEEE J. Solid-State Circuits*, vol. 39, no. 9, pp. 1415–1424, Sep. 2004.
[21] X. Xie *et al.*, "Low-noise and broadband optical frequency comb generation based on an optoelectronic oscillator," *Opt. Lett.*, vol. 39, no. 4, pp. 785–788, Feb. 2014.
[22] X. S. Yao and L. Maleki, "Multiloop optoelectronic oscillator," *IEEE J. Quantum Electron.*, vol. 36, no. 1, pp. 79–84, Jan. 2000.
[23] S. Xiao, L. Hollberg, N. R. Newbury, and S. A. Diddams, "Toward a low-jitter 10 GHz pulsed source with an optical frequency comb generator," *Opt. Exp.*, vol. 16, no. 12, pp. 8498–8508, Jun. 2008.
[24] L. Paciorek, "Injection locking of oscillators," *Proc. IEEE*, vol. 53, no. 11, pp. 1723–1727, Nov. 1965.
[25] S. Kalia, M. Elbadry, B. Sadhu, S. Patnaik, J. Qiu, and R. Harjani, "A simple, unified phase noise model for injection-locked oscillators," in *Proc. Int. Symp. IEEE Radio Freq. Integr. Circuits*, Baltimore, MD, USA, 2011, pp. 1–4.
[26] H. Peng *et al.*, "Tunable DC-60 GHz RF generation utilizing a dual-loop optoelectronic oscillator based on stimulated Brillouin scattering," *J. Lightw. Technol.* vol. 33, no. 13, pp. 2707–2715, Jul. 2015.